Supporting Information for ”Statistics and Forecasting of Aftershocks during the 2019 Ridgecrest, California, Earthquake Sequence”

Robert Shcherbakov[1,2] *

[1]Department of Earth Sciences, University of Western Ontario, London, Ontario, *N6A 5B7*, Canada.

[2]Department of Physics and Astronomy, University of Western Ontario, London, Ontario, *N6A 3K7*, Canada.

Contents of this file

1. Figures S1 to S15
2. Tables S1 to S3

*E-mail: rshcherb@uwo.ca

Introduction

The Supporting Information for this article includes Tables S1-S3 with the parameters of the Gamma distribution, which was used as a prior distribution for the parameters of the three models considered in the work. It also includes plots illustrating the fit of the compound OU (Figure S1) and the ETAS (Figure S2) models. The MCMC sampling of the model parameters for the OU (Figures S4-S5), the compound OU (Figures S6-S8), the ETAS (Figures S9-S11) models are provided for one specific training and forecasting time intervals. The additional quantile scores of the plots are given in Figures S12-S15.

The data analysis was performed using a computer code written in Matlab.

List of figures

The compound Omori-Utsu (OU) model

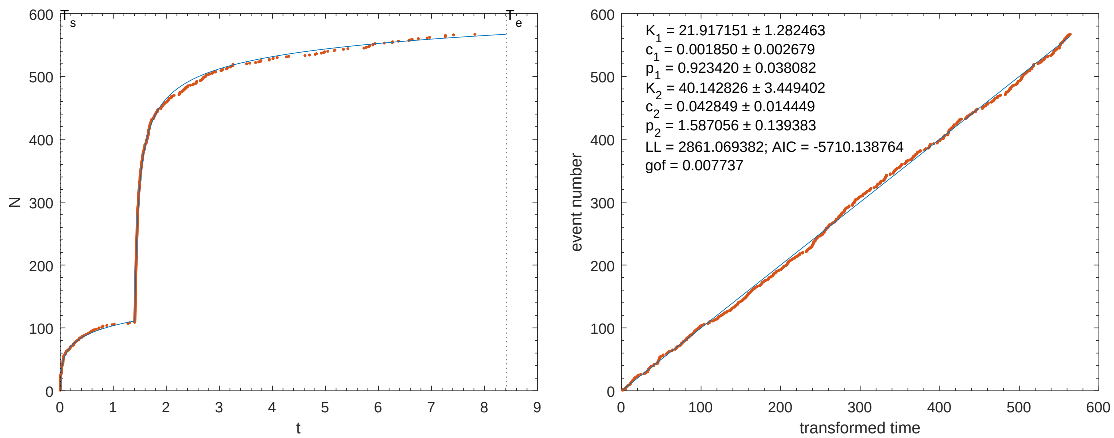

Figure S1. The fitting of the compound Omori-Utsu law, equation (5), to the 2019 Ridgecrest sequence. $T_0 = 0$ corresponds to the occurrence of M6.4 foreshock on 2019/07/04 (17:33:49 UTC). a) The cumulative number of earthquakes is plotted as solid symbols. The corresponding fit of the compound Omori-Utsu law to the cumulative numbers is given as solid curve during the time interval $[T_0, T_e] = [0, 8.407]$ days. This includes 7 days of aftershocks after the M7.1 mainshock. b) The number of earthquakes is plotted in transformed time. All earthquakes above magnitude $m \geq 3.2$ were used.

The Epidemic Type Aftershock Sequence (ETAS) model

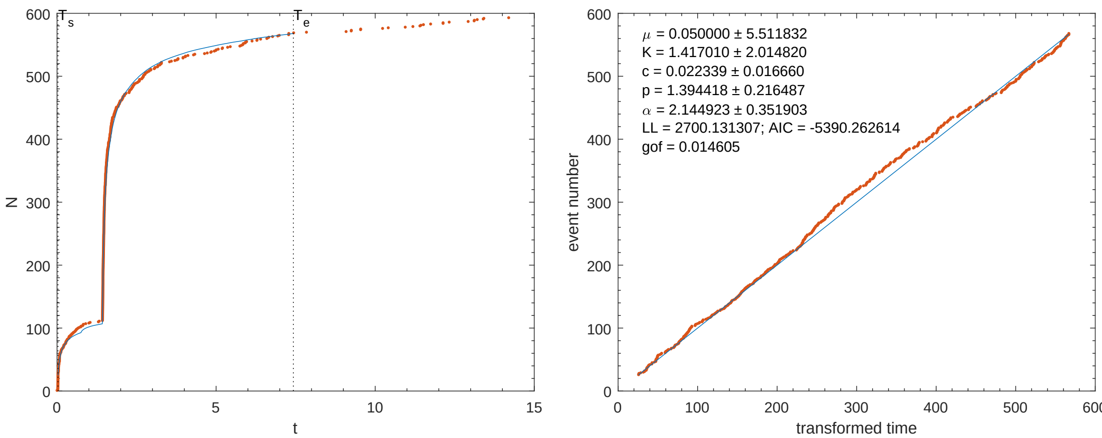

Figure S2. The fitting of the ETAS model, equation (6), to the 2019 Ridgecrest sequence. $T_0 = 0$ corresponds to the occurrence of M3.98 foreshock on 2019/07/04 (17:02:55 UTC). a) The cumulative number of earthquakes is plotted as solid symbols. The corresponding fit of the ETAS model to the cumulative numbers is given as solid curve during the time interval $[T_s, T_e] = [0.03, 8.428]$ days. This includes 7 days of aftershocks after the M7.1 mainshock. b) The number of earthquakes is plotted in transformed time. All earthquakes above magnitude $m \geq 3.2$ were used.

Markov Chain Monte Carlo sampling

The Omori-Utsu (OU) model parameters

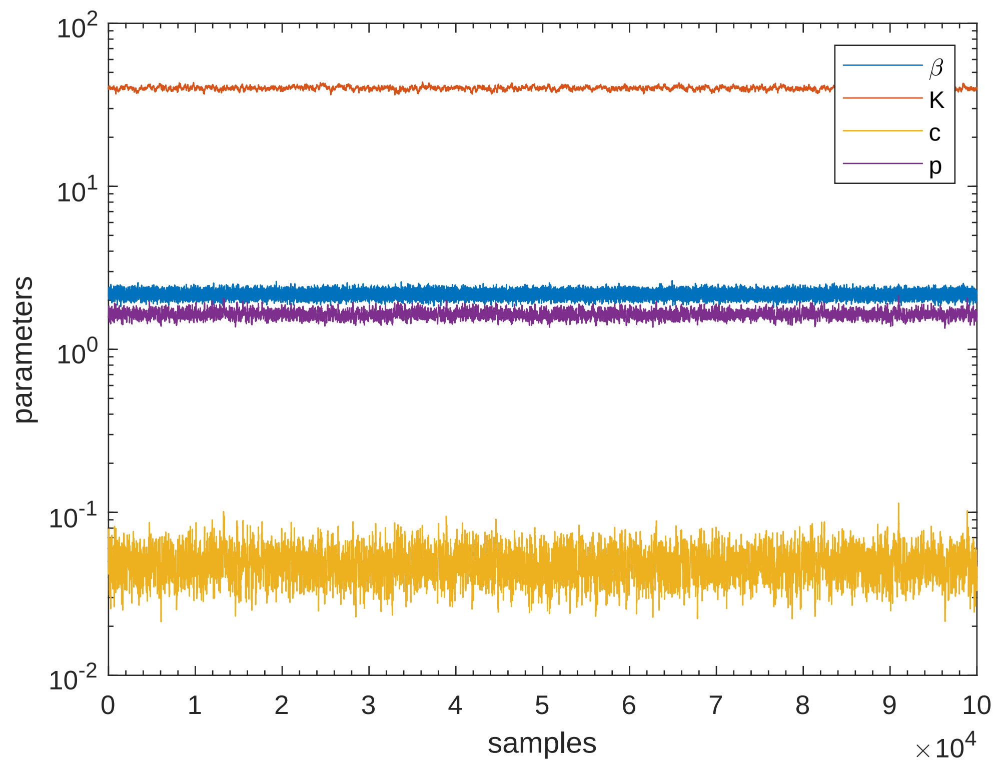

Figure S3. The MCMC chains of the OU model parameters sampled from the posterior distribution for the Ridgecrest sequence during one day of aftershocks above magnitude $m_c = 3.2$ and starting from the occurrence of the M7.1 mainshock. The total number of MCMC 200,000 steps were generated and 100,000 steps were discarded as burn-in.

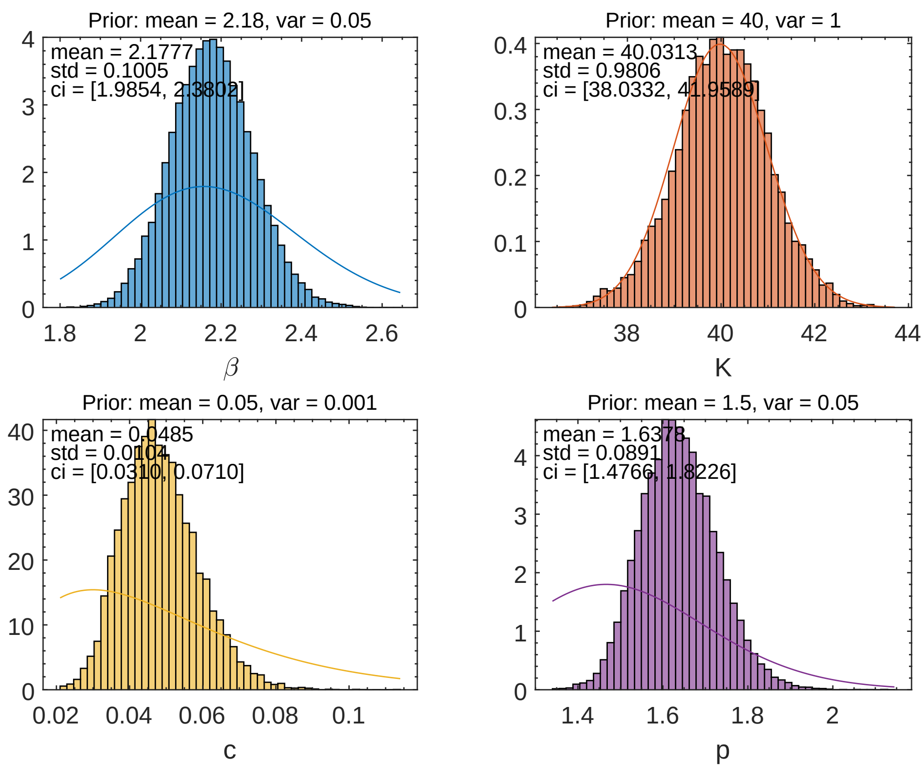

Figure S4. The distribution of the OU model parameters computed from the MCMC chains given in Figure S3. The corresponding mean, standard deviation, and 95% Bayesian confidence bounds for the parameters are provided in the legend. The solid curves represent the prior Gamma distribution for each model parameter.

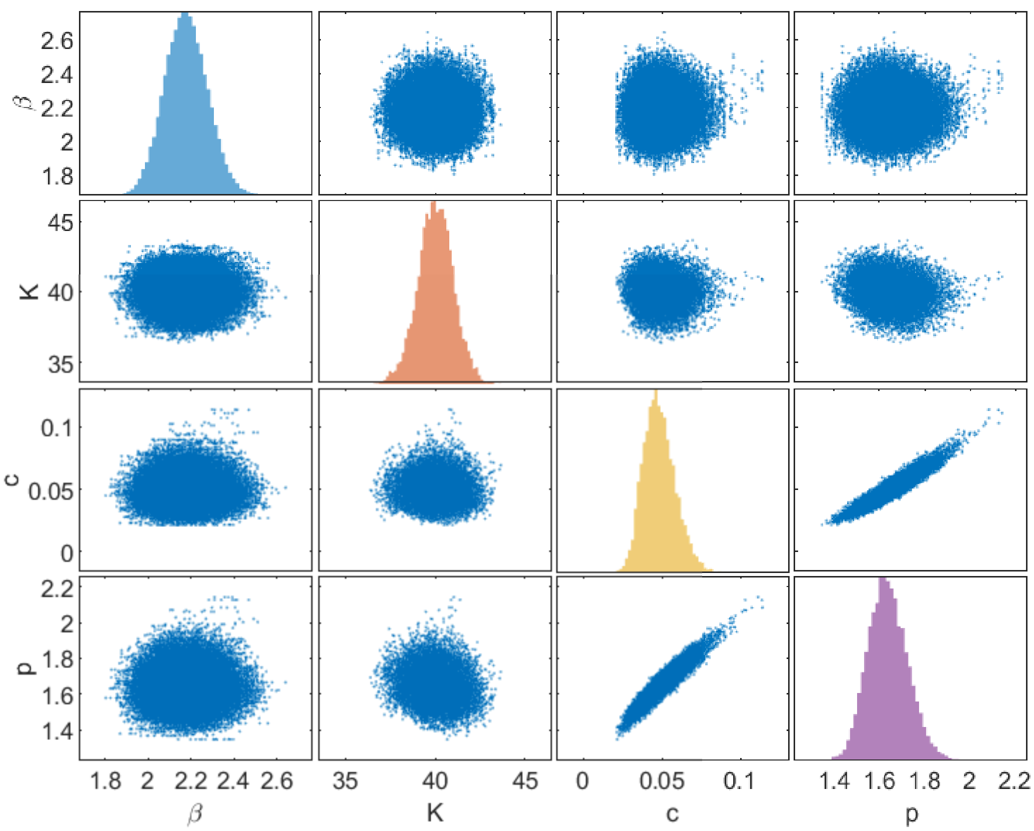

Figure S5. The matrix plot of the pairs of the OU model parameters computed from the MCMC chains given in Figure S3 and showing the correlation structure of the parameters.

The compound OU model parameters

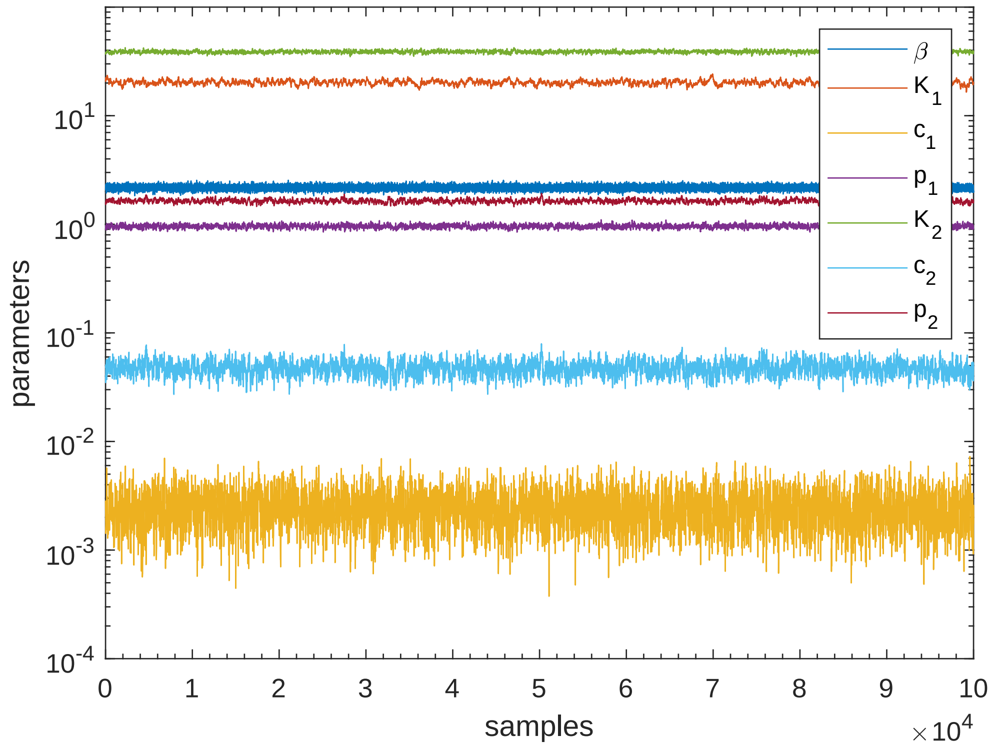

Figure S6. The MCMC chains of the compound OU model parameters sampled from the posterior distribution for the Ridgecrest sequence during $[T_0, T_e] = [0, 2.407]$ target time interval with aftershocks above magnitude $m_c = 3.2$ and starting from the occurrence of the M6.4 foreshock. The total number of MCMC 200,000 steps were generated and 100,000 steps were discarded as burn-in.

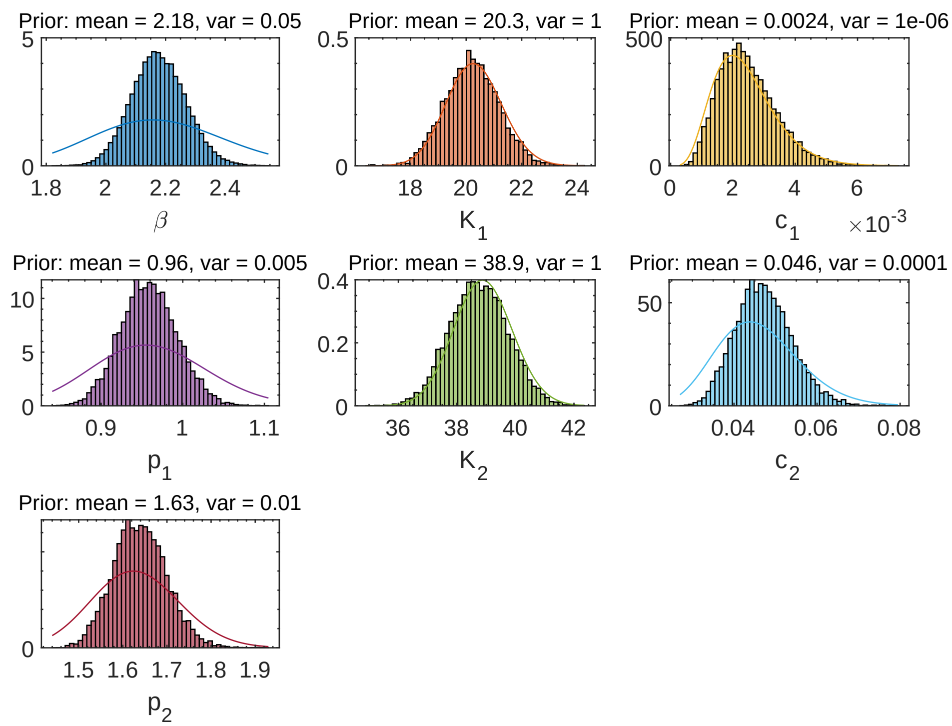

Figure S7. The distribution of the compound OU model parameters computed from the MCMC chains given in Figure S6. The corresponding mean, standard deviation, and 95% Bayesian confidence bounds for the parameters are provided in the legend. The solid curves represent the prior Gamma distribution for each model parameter.

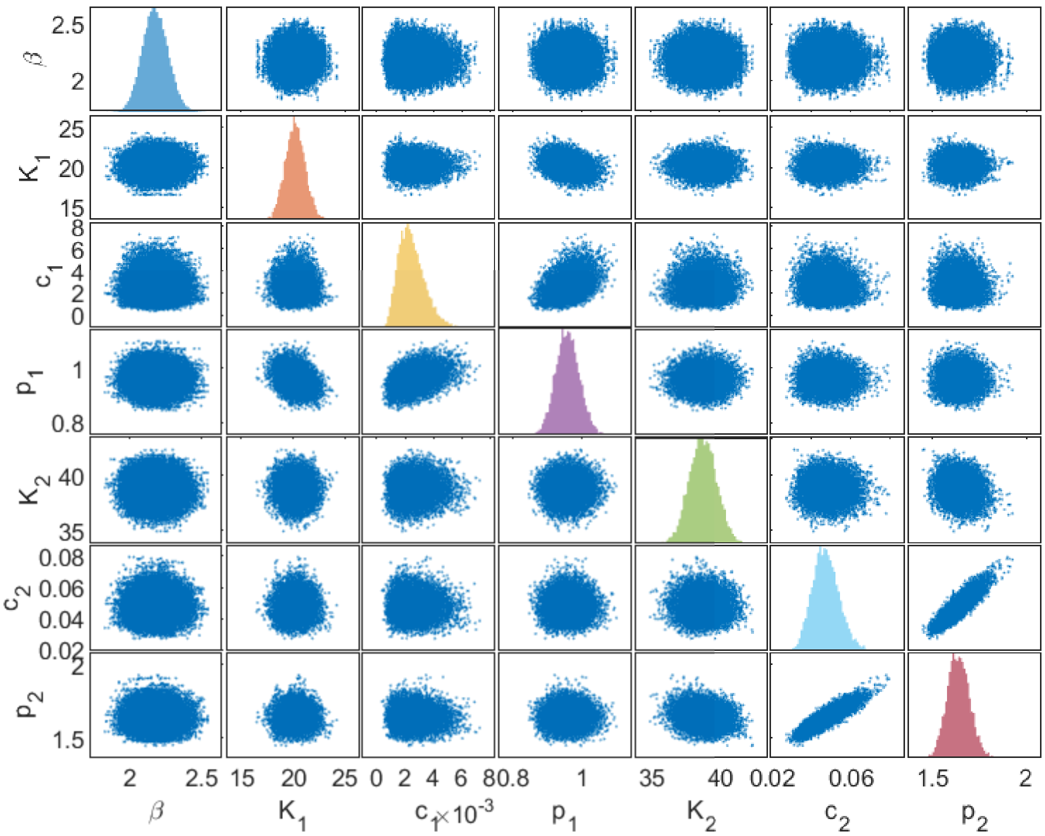

Figure S8. The matrix plot of the pairs of the compound OU model parameters computed from the MCMC chains given in Figure S6 and showing the correlation structure of the parameters.

The ETAS model parameters

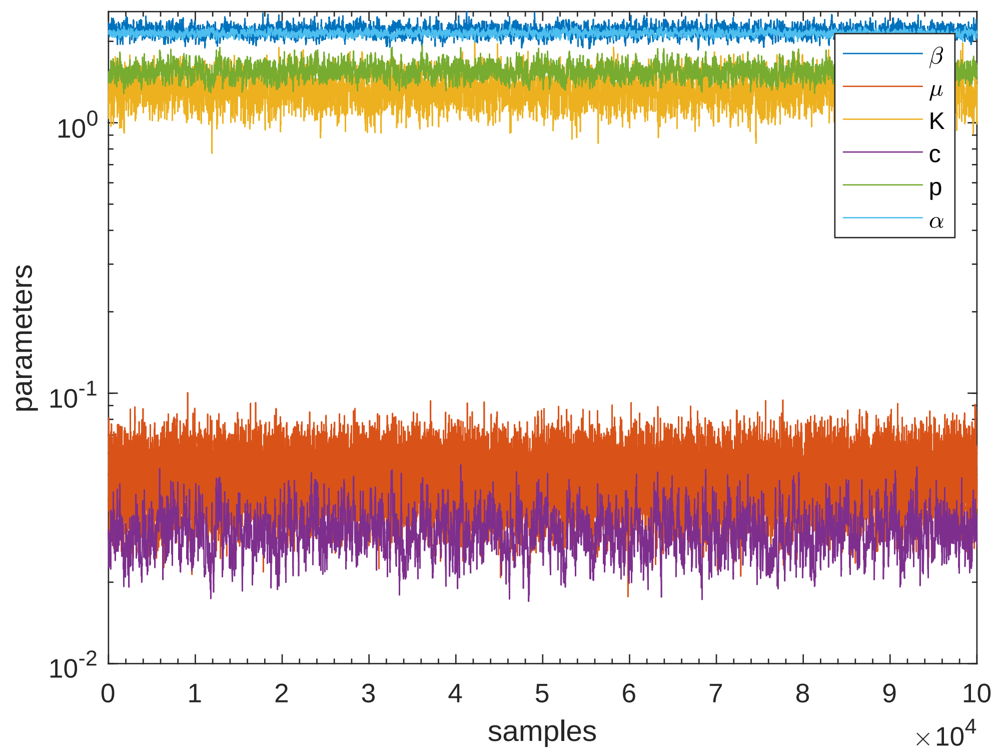

Figure S9. The MCMC chains of the ETAS parameters sampled from the posterior distribution for the 2019 Ridgecrest sequence $[T_s, T_e] = [0.03, 2.428]$ target time interval with aftershocks above magnitude $m_c = 3.2$ and starting from the occurrence of the M6.4 foreshock. The total number of 150,000 steps were generated and 50,000 steps were discarded as burn-in.

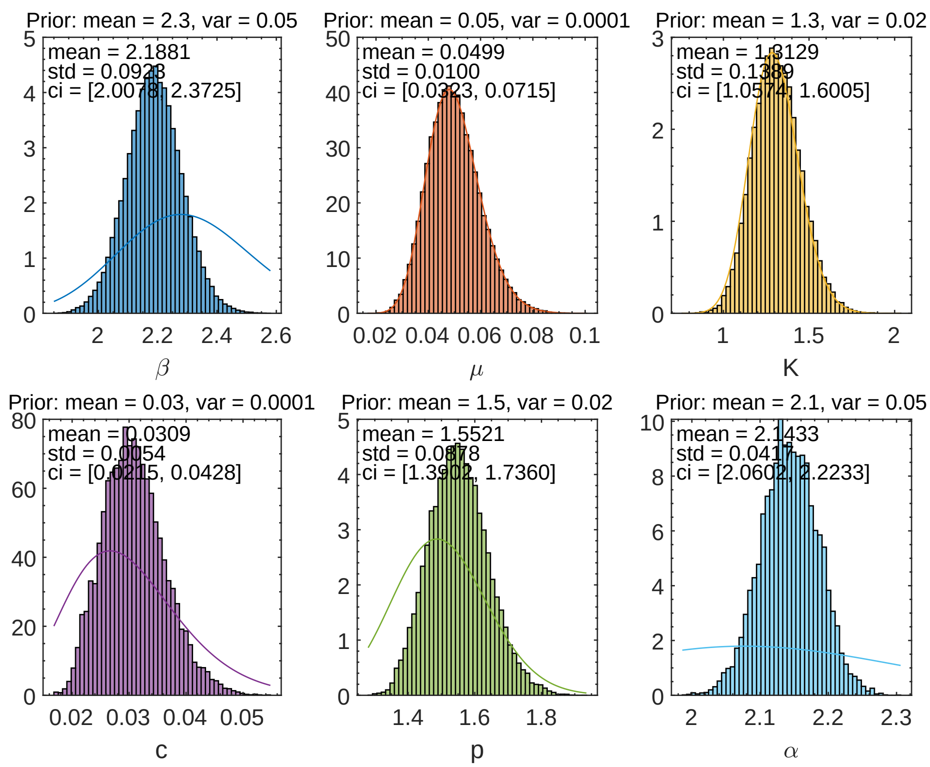

Figure S10. The distribution of the ETAS parameters computed from the MCMC chains given in Figure S9. The corresponding mean, standard deviation, and 95% Bayesian confidence bounds for the parameters are provided in the legend. The solid curves represent the prior Gamma distribution for each model parameter.

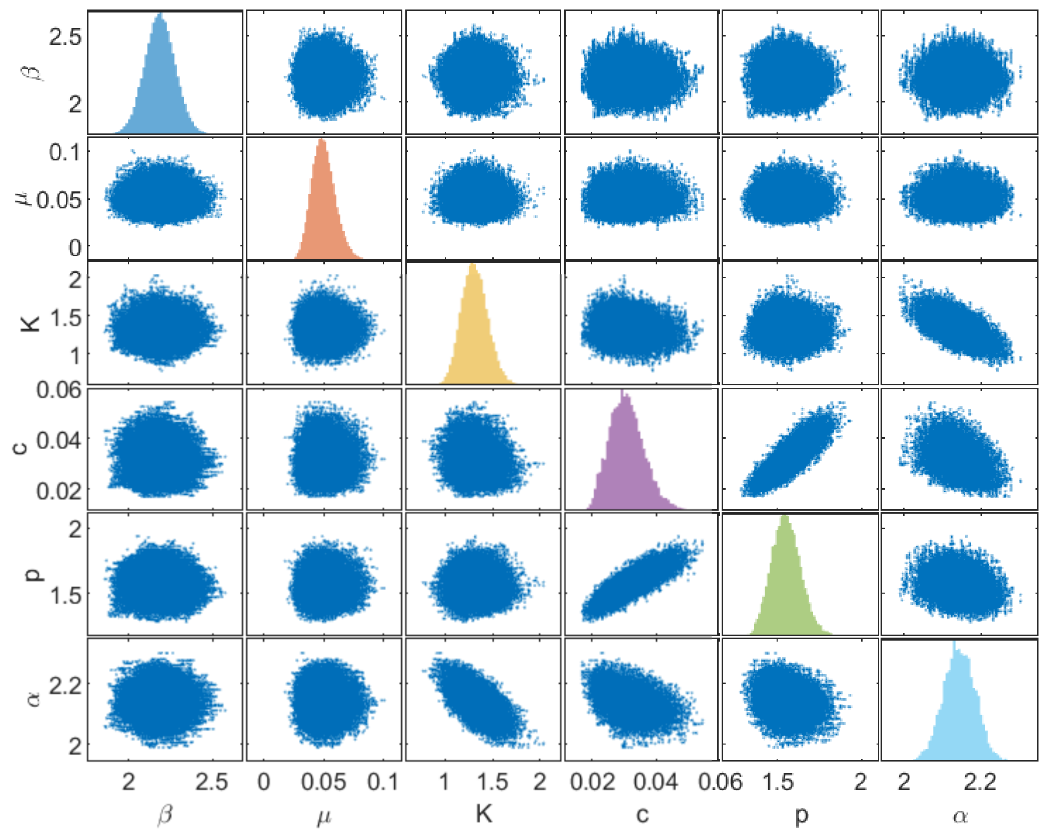

Figure S11. The matrix plot of the pairs of the ETAS parameters computed from the MCMC chains given in Figure S9 and showing the correlation structure of the simulated parameters.

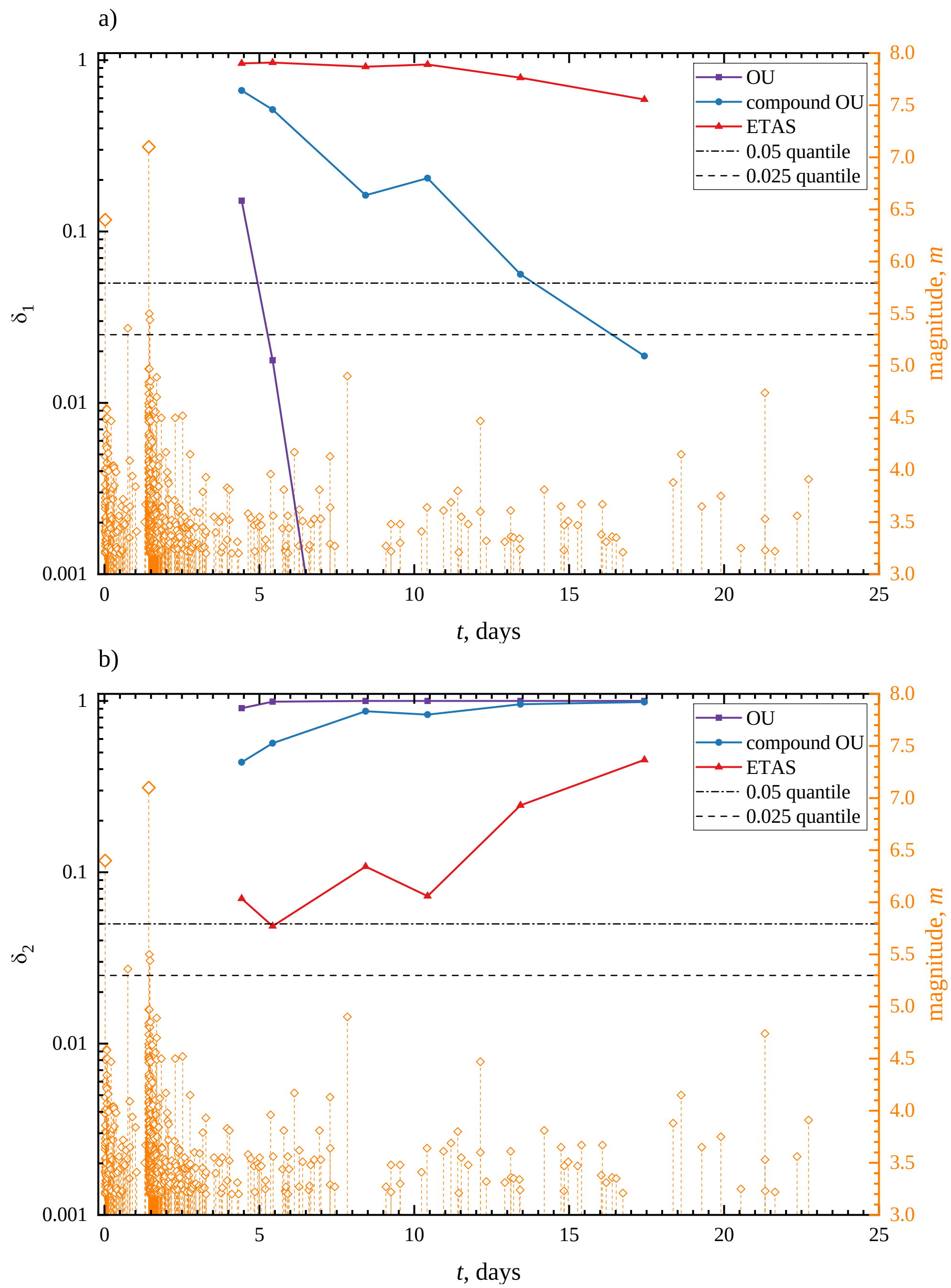

Figure S12. Plot of the quantile scores a) δ_1 (N-test), b) δ_2 (N-test), and c) κ (M-test) for the performance of the aftershock forecasts based on the three point process models. The scores are computed at the end of each forecasting time interval. The end of the training time interval is fixed at $T_e = 3.428$ days while the forecasting time interval is increasing as $\Delta T = 1, 2, 5, 7, 10, 14$.

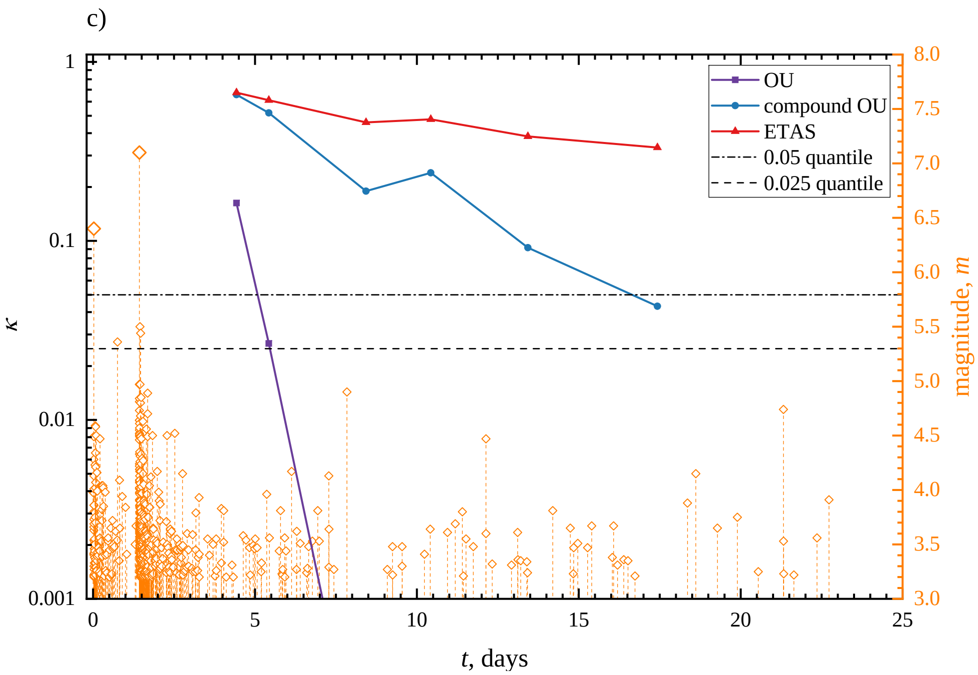

Figure S12. Continued.

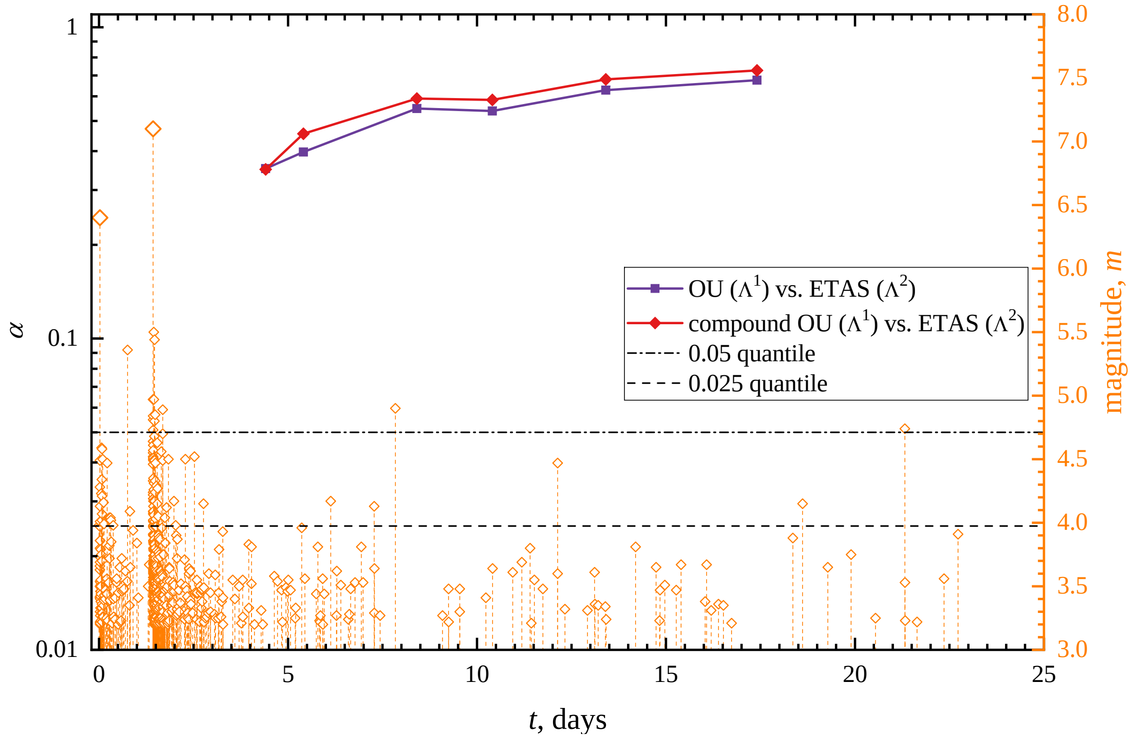

Figure S13. Plot of the quantile score α (R-test) for the comparative test of the ETAS model versus the forecast based on the OU model and on the compound OU model. The scores are computed at the end of each forecasting time interval as in Figure S12.

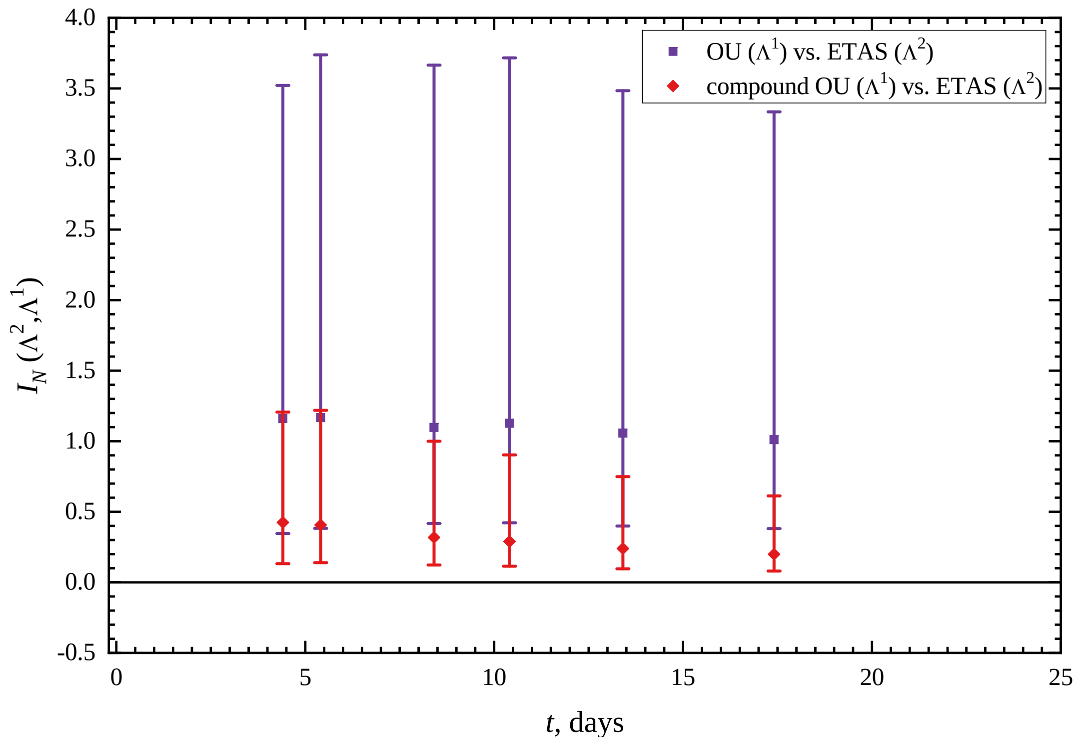

Figure S14. The sample information gain for the pairs of the models. The solid squares correspond to the comparison of the forecasts based on the ETAS model versus the forecasts based on the OU model. The solid diamonds correspond to the comparison of the forecasts based on the ETAS model versus the forecast based on the compound OU model. The 95% confidence intervals are given.

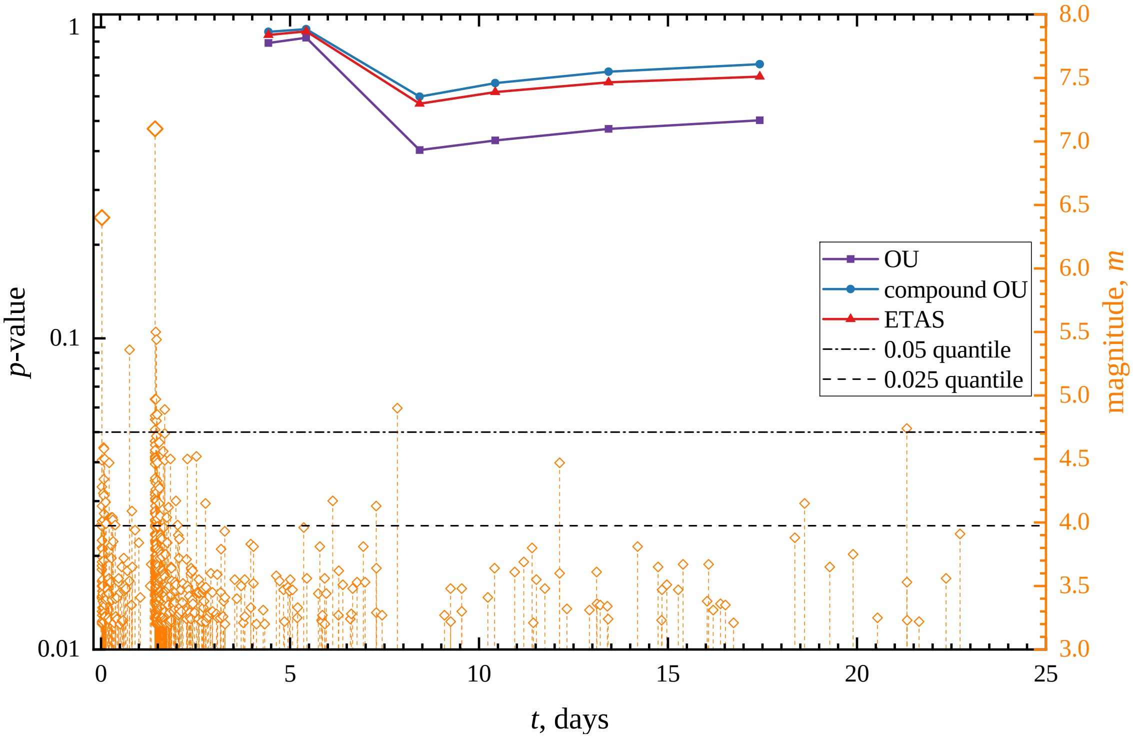

Figure S15. Plot of the Bayesian predictive distribution p-value for the three models. The p-values are computed at the end of each forecasting time interval as in Figure S12.

Tables for the model prior parameters

The Omori-Utsu model

Table S1. Summary of the parameters used for the prior distribution of the OU model $\{\theta,\,\omega\} = \{\beta,\,K_{\mathrm{o}},\,c_{\mathrm{o}},\,p_{\mathrm{o}}\}$. For the priors $\pi(\{\theta,\omega\})$ the Gamma distribution was used with the mean and variance specified for each parameter.

Prior for	β	K_{o}	c_{o}	p_{o}
mean	2.18	40.0	0.05	1.5
Var	0.05	1.0	1e-3	0.05

The compound Omori-Utsu model

Table S2. Summary of the parameters used for the prior distribution of the compound OU model $\{\theta,\,\omega\} = \{\beta,\,K_1,\,c_1,\,p_1,\,K_2,\,c_2,\,p_2\}$. For the priors $\pi(\{\theta,\omega\})$ the Gamma distribution was used with the mean and variance specified for each parameter.

Prior for	β	K_1	c_1	p_1	K_2	c_2	p_2
mean	2.18	20.3	0.0024	0.96	38.9	0.046	1.63
Var	0.05	1.0	1e-6	0.005	1.0	1e-4	0.01

The Epidemic Type Aftershock Sequence (ETAS) model

Table S3. Summary of the parameters used for the prior distribution of the ETAS model $\{\theta,\,\omega\} = \{\beta,\,\mu,\,K,\,c,\,p,\,\alpha\}$. For the priors $\pi(\{\theta,\omega\})$ the Gamma distribution was used with the mean and variance specified for each parameter.

Prior for	β	μ	K	c	p	α
mean	2.3	0.05	1.3	0.03	1.5	2.1
Var	0.05	1e-4	0.02	1e-4	0.02	0.05